

# Star formation

Protostellar evolution and Pre-Main-Sequence  
Phase

# Protostellar evolution

- Isothermal collapse up to densities of  $\sim 10^{10} \text{ cm}^{-3}$
- Then the dust becomes optically thick
  - Center warms up, fragmentation stops  
→ **1<sup>st</sup> hydrostatic core**
- Slow, adiabatic evolution
  - Temperature increases
  - Density increase very slow
- Infalling gas shock dominates luminosity

$$L_{shock} = \frac{G M_* \dot{M}}{R_*}$$

# Protostellar evolution

- When  $T \sim 1000$  K, dust evaporates  
→ “opacity gap”
- When the  $T \sim 2000$  K,  $H_2$  dissociates
  - Dissociation of  $H_2$  “consumes” significant amount of energy (4.48 eV per  $H_2$ )
  - Temperature remains approximately constant  
**2<sup>nd</sup> collapse**
- At  $T > 3000$  K hydrogen is ionized
  - Gas turns optically thick  
→ **2<sup>nd</sup> hydrostatic core**

# Evolution of the protostellar core

- Evolution of density <sub>318</sub> - central temperature

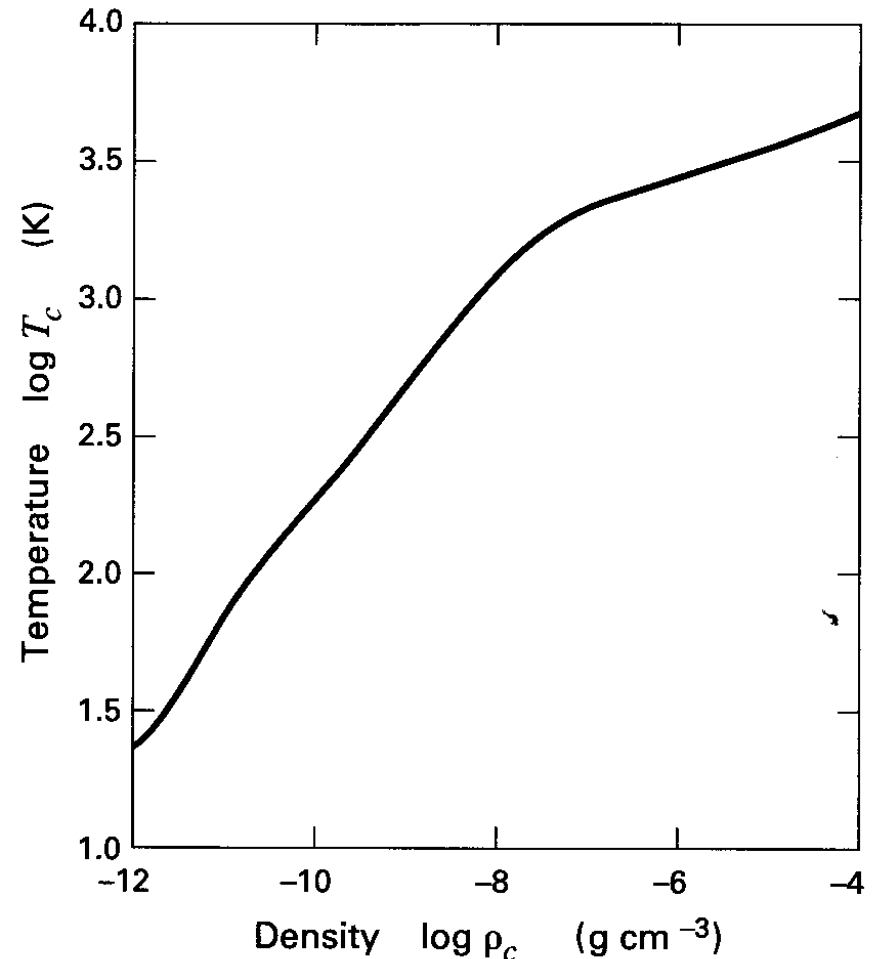
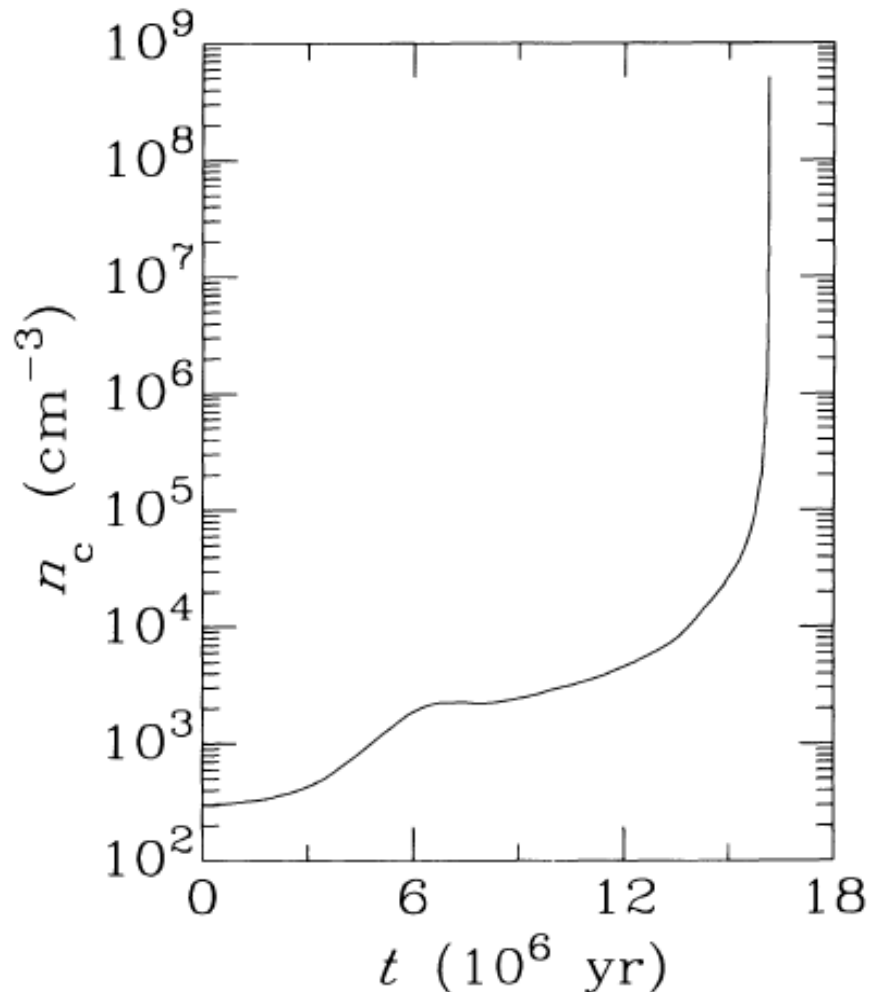


FIG. 1a.—Evolution of central values of model 1. Density  $n_c$  (in  $\text{cm}^{-3}$ ) as a function of time  $t$  (in  $10^6$  yr).

# Protostar

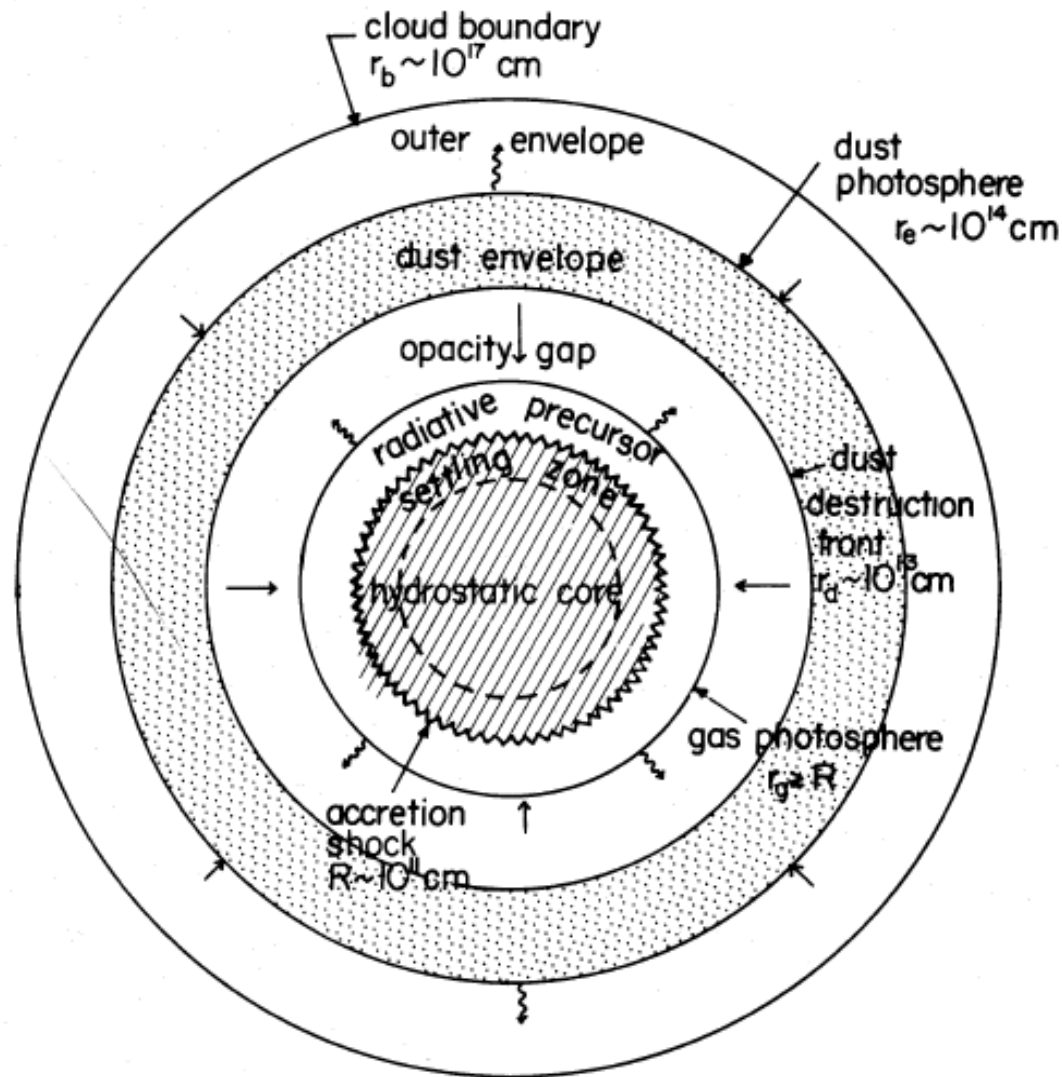


FIG. 1.—The structure of a protostar in the main accretion phase. The dimensions for the various features are given very roughly to aid visualization of the many orders of magnitude of scale involved in this complex problem.

# Protostar

- Opacity gap separates inner core and outer shell
  - Separate physical evolution
- Accretion shock at both “surfaces”
- Evolution of outer shell:
  - Determined by accretion rate
  - Radiation from accretion shock
  - No contribution to heating
- Evolution of core:
  - Stellar problem
  - Temperature increase up to fusion
  - Chemical evolution

# Accretion

- Mass gaining core whose luminosity stems mainly from external accretion.

$$L_{acc} = \frac{G M_* \dot{M}}{R_*} \approx 60 L_{\odot} \left| \frac{\dot{M}}{10^{-5} M_{\odot} \text{ yr}^{-1}} \right| \left| \frac{M_*}{1 M_{\odot}} \right| \left| \frac{R_*}{5 R_{\odot}} \right|^{-1}$$

- Typical rates:  $10^{-5} \dots 10^{-3} M_{\odot}/\text{a}$   
 $\rightarrow 10^2 \dots 10^4 L_{\odot}$
- **But:** Protostars are *invisible* in the optical

# Accretion

Growth of radius follows a fixed curve set by hydrostatic core physics and accretion rate

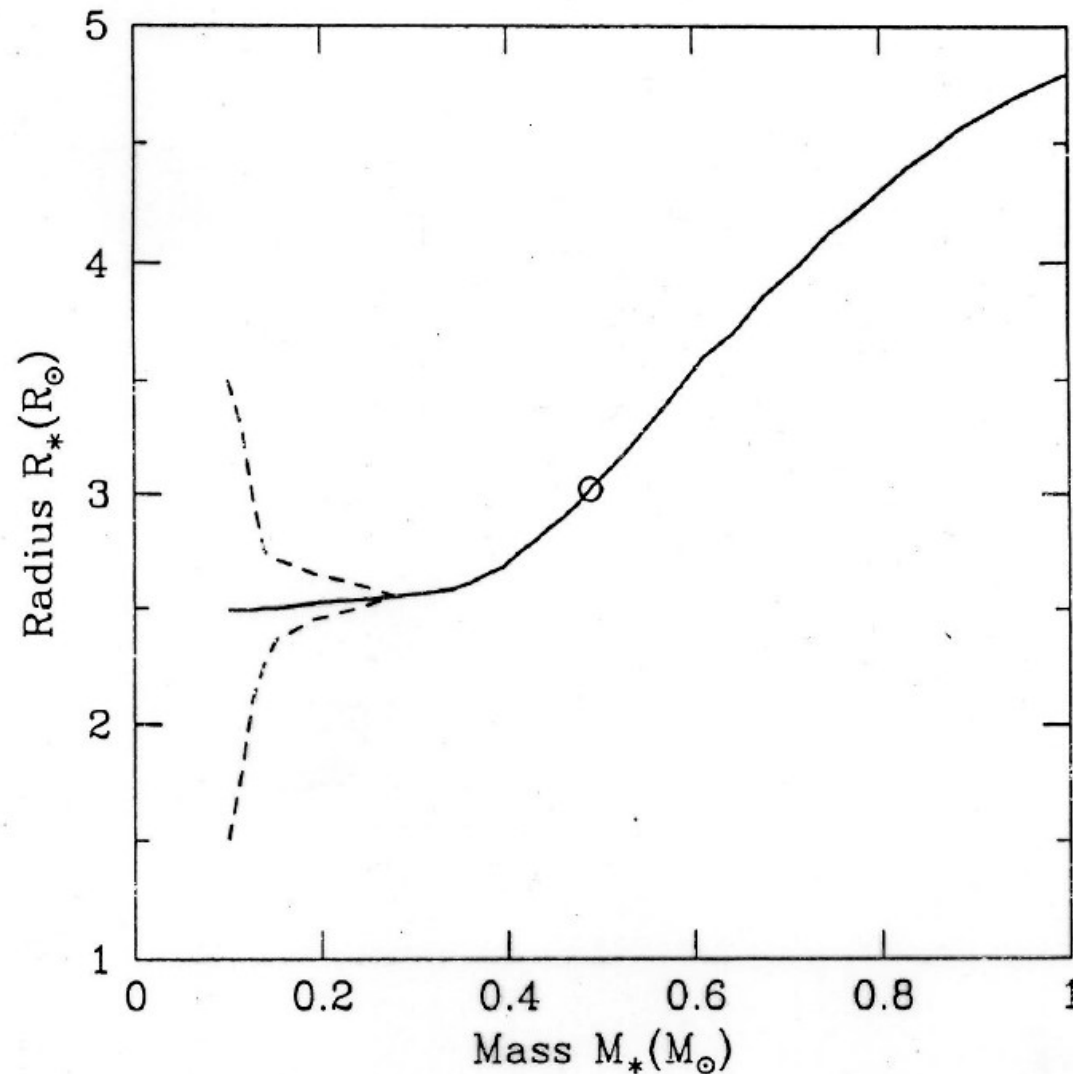


**Fig. 4.** Mass radius relation for a protostar accreting at  $\dot{M} = 10^{-5} M_\odot \text{ yr}^{-1}$ . As shown by the dashed curves, different initial radii quickly converge to the same mass-radius relation. The circle marks the onset of full convection. (From Stahler [47])



# Accretion

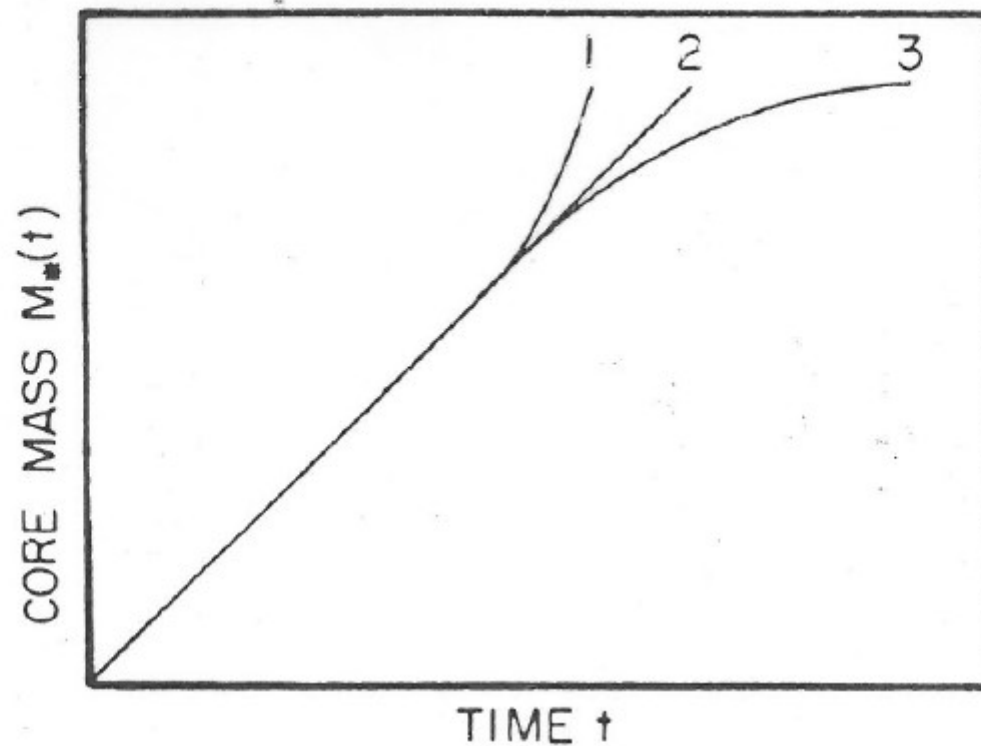


FIG. 2.—The growth of the mass of the central hydrostatic core. Curve 2 illustrates a case of a constant mass accretion rate, such as that obtained for the collapse of a singular isothermal sphere when outer boundary conditions are ignored. Curve 1 gives a schematic increase in  $\dot{M}$  in the late stages because of the application of a constant pressure at the outer boundary, while curve 3 gives a schematic decrease because of the requirement of a constant volume.

# Surface temperature

- radiates like a blackbody with a temperature given by the Stefan-Boltzmann law

$$4 \pi R_*^2 \sigma_B T_{eff}^4 \approx L_{acc}$$

$$T_{eff} \approx \left( \frac{G M_* \dot{M}}{4 \pi \sigma_B R_*^3} \right)^{1/4}$$

$$T_{eff} \approx 7300 \text{ [K]} \left( \frac{\dot{M}}{10^{-5} M_\odot \text{ yr}^{-1}} \right)^{1/4} \left( \frac{M_*}{1 M_\odot} \right)^{1/4} \left( \frac{R_*}{5 R_\odot} \right)^{-3/4}$$

# Outer temperature

- This radiation (of a stellar-like photosphere) is transmitted through the opacity gap, absorbed by the dust and re-radiated at the dust photosphere
- like a black body with an approximate temperature of 300 K
- radius 14 AU

# Accretion shock

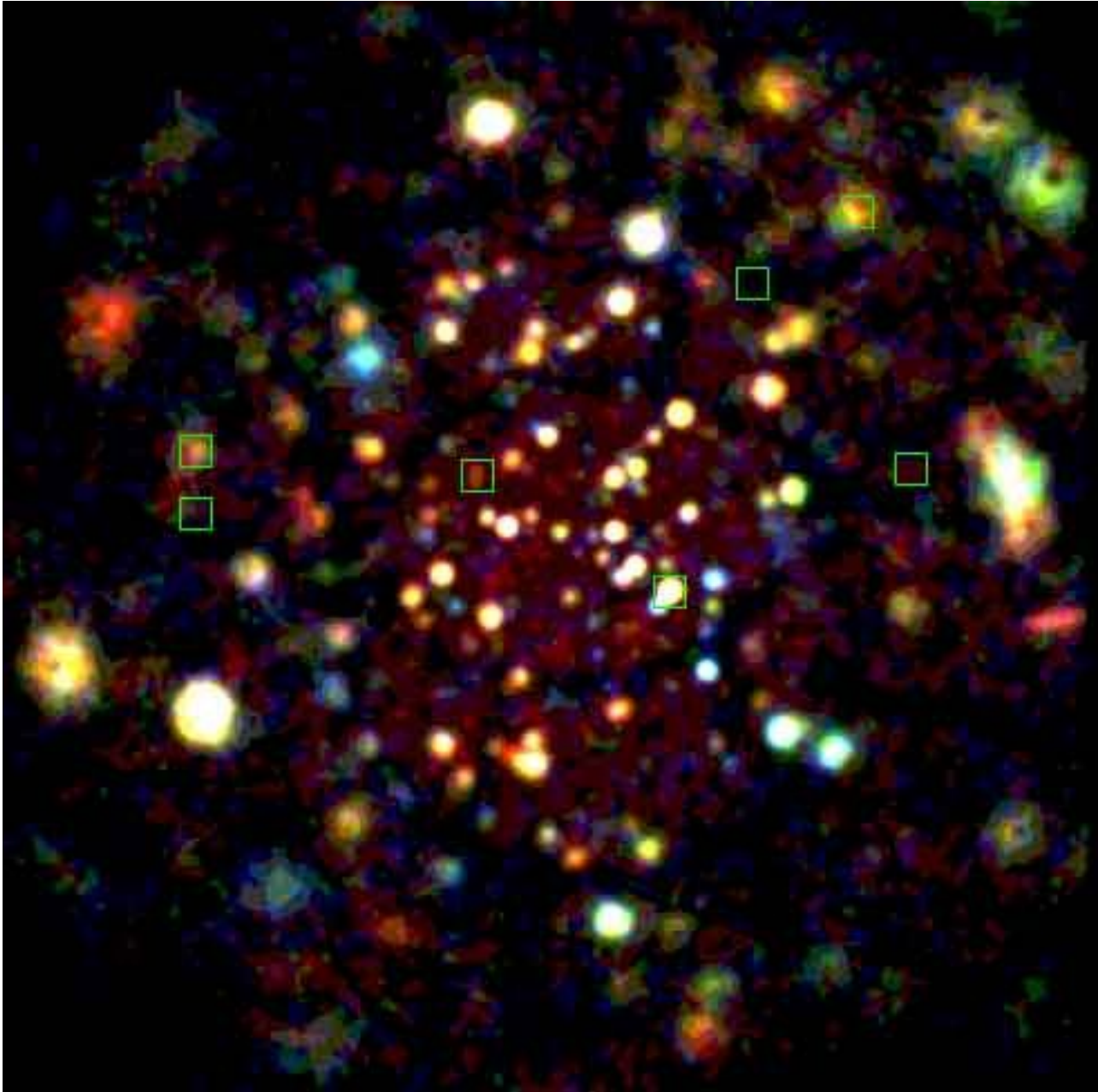
- Accretion velocity

$$v_{ff} = \sqrt{\frac{2 G M_*}{R_*}} = 280 [\text{km s}^{-1}] \left( \frac{M_*}{1 M_\odot} \right)^{1/2} \left( \frac{R_*}{5 R_\odot} \right)^{-1/2}$$

= supersonic!

- Creates temperature jump on impact  
→ hot relaxation zone
- postshock temperatures in excess of  $10^6$  K
- UV and X-ray photons (absorbed in opaque, ionized) radiative precursor

# Accretion shock



X-ray image of the Pleiades taken by ROSAT.

The 7 squares show the optically visible stars.

# Accretion shock

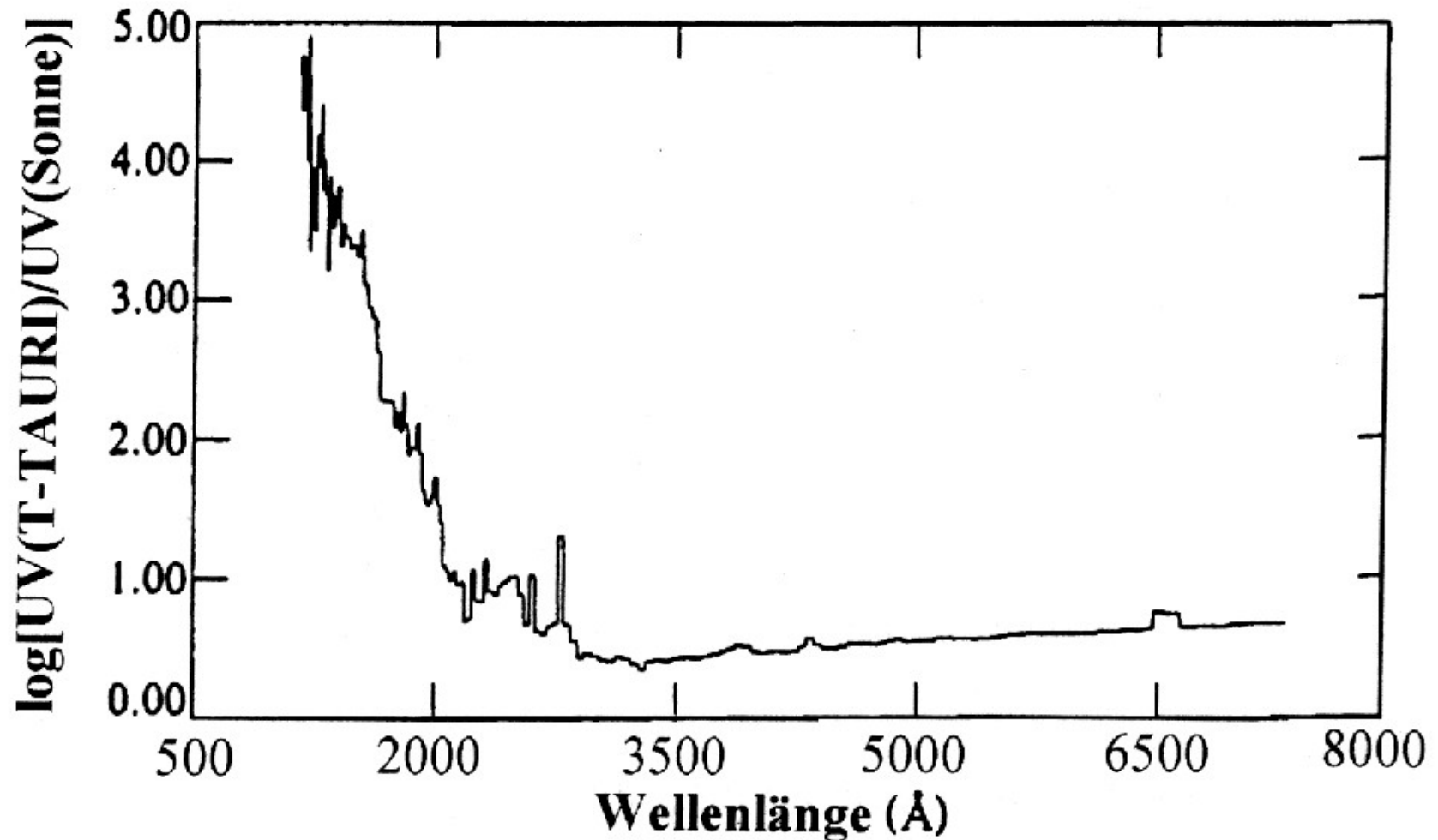


**Abbildung 7.4:** Die spektrale Intensität eines T-Tauri-Sternes im Verhältnis zu derjenigen der heutigen Sonne.

# Evolution of the protostellar core

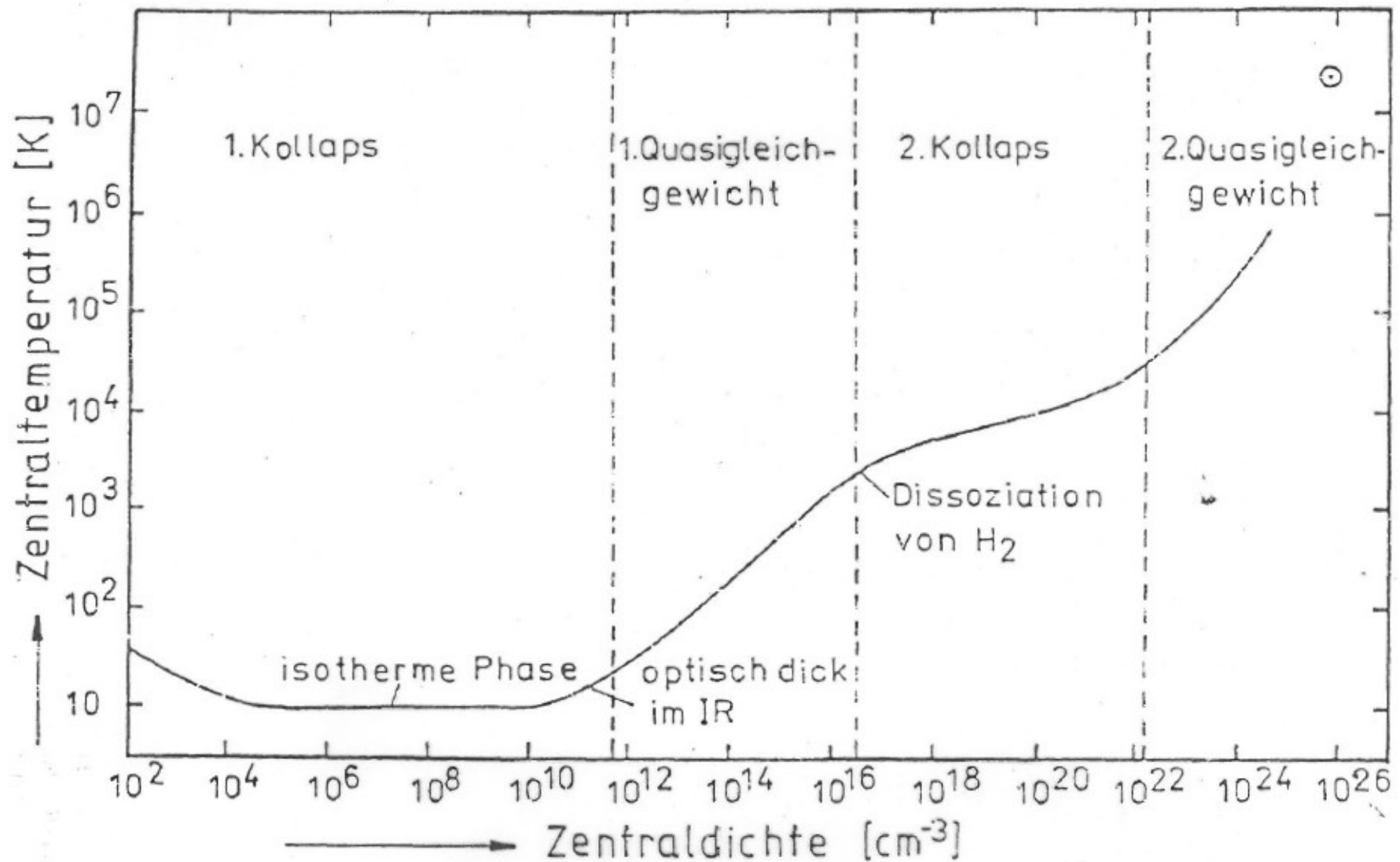


Abbildung 6.3: Zusammenhang zwischen Temperatur und Dichte im Zentrum einer kugelsymmetrischen Wolke während des protostellaren Kollaps'.



# Hertzsprung-Russell diagram

## First steps:

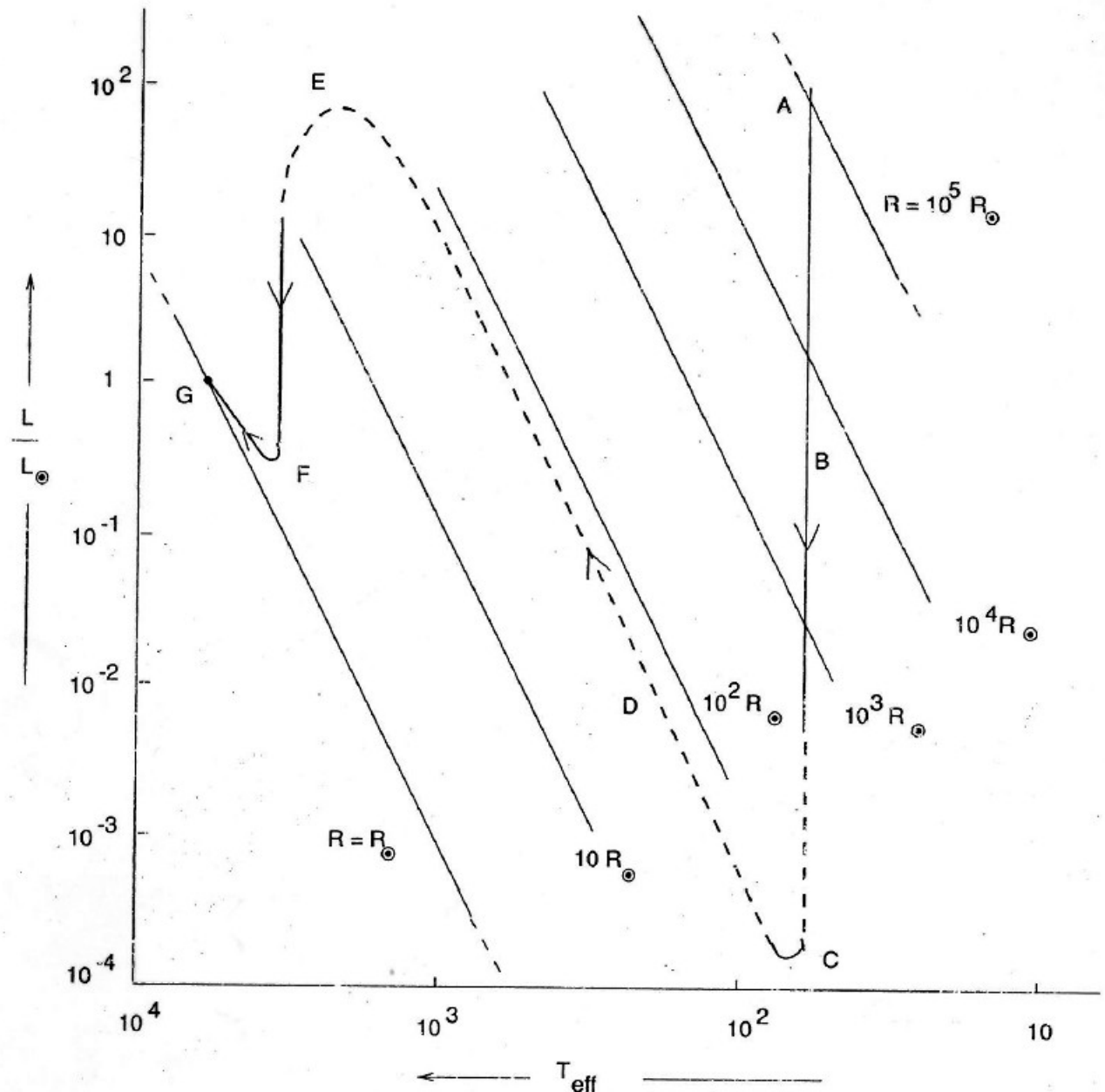
## isothermal collapse:

→ Hayashi tracks

- Decreasing radius
- Constant temperature

## hydrostatic cores:

- Adiabatic heating up
- Luminosity driven by accretion/collapse
- Supported by D-burning





# The Pre-Main-Sequence phase

- The main accretion phase is finished. Accretion is not dominant anymore, i.e. almost final mass is already achieved.
- The envelope is dispersed, so the star becomes visible in the optical.
- The central temperature is not yet high enough to start hydrogen burning.

**Pre-Main-Sequence Stars** are slowly contracting objects of fixed mass, for which luminosity stems from gravitational contraction.

# The birthline

- Point in HR diagram where the youngest stars become visible, at the transition between protostellar phase and pre-main sequence phase.

$$L = 4\pi R_*^2 \sigma_B T_{\text{eff}}^4$$

- During the protostellar phase:
  - **Luminosity** and  $T_{\text{eff}}$  are set by infall dynamics

$$L_{\text{acc}} = \frac{GM_* \dot{M}}{R_*} = 61 L_{\text{sun}} \left( \frac{\dot{M}}{10^{-5} M_{\text{sun}} \text{yr}^{-1}} \right) \left( \frac{M_*}{1 M_{\text{sun}}} \right) \left( \frac{R_*}{5 R_{\text{sun}}} \right)^{-1}$$

$$T_{\text{eff}} = \left( \frac{GM_* \dot{M}}{4\pi \sigma_B R_*^3} \right)^{1/4} \approx 7300 \text{ [K]} \left( \frac{\dot{M}}{10^{-5} M_{\text{sun}} \text{yr}^{-1}} \right)^{1/4} \left( \frac{M_*}{1 M_{\text{sun}}} \right)^{1/4} \left( \frac{R_*}{5 R_{\text{sun}}} \right)^{-3/4}$$

- For a given mass, the **radius** is determined by internal structure (balance of self-gravity and thermal pressure) [stays true during PMS phase]

# The birthline

The birthline is  
model dependent

depends on the  $R(M)$   
Relation at the end of  
protostellar phase

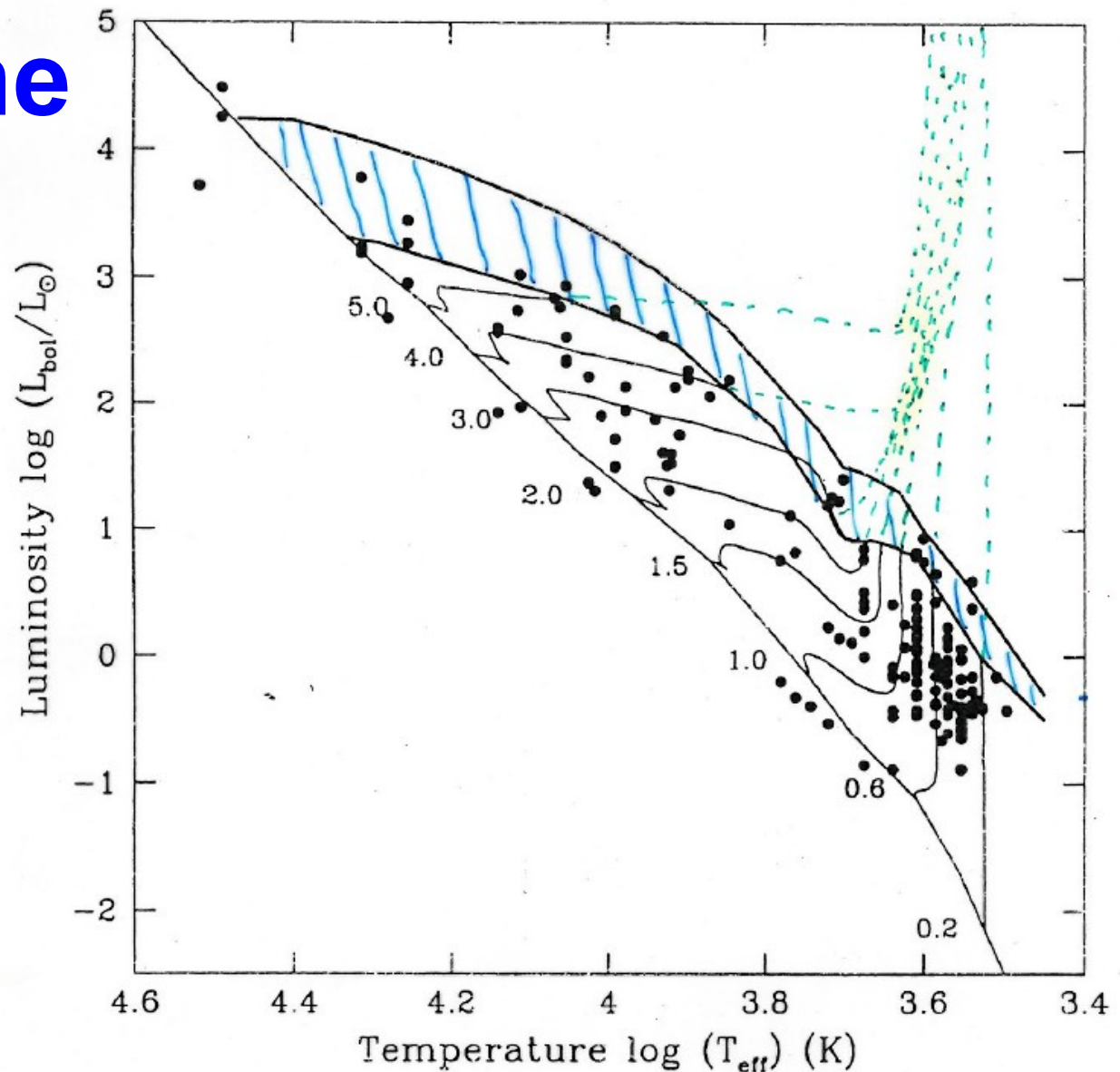
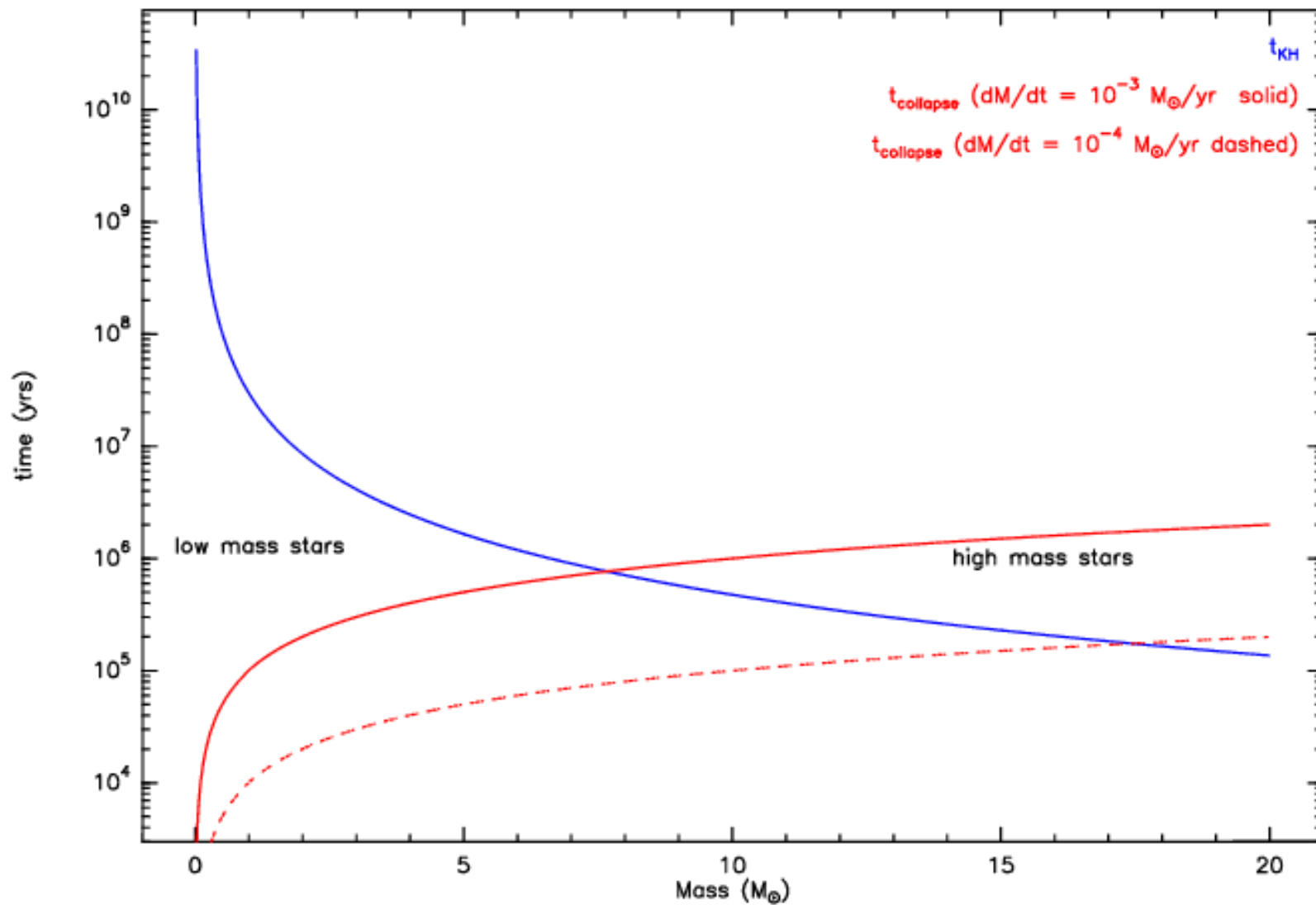


**Fig. 7.** Location of the stellar birthline in the H-R diagram for accretion rates of  $10^{-5}$  (lower heavy curve) and  $10^{-4}$  (upper heavy curve)  $M_{\odot} \text{ yr}^{-1}$ . Symbols give the positions of young PMS stars. Labeled curves are PMS evolutionary tracks for the indicated stellar mass. (From Palla & Stahler [41])

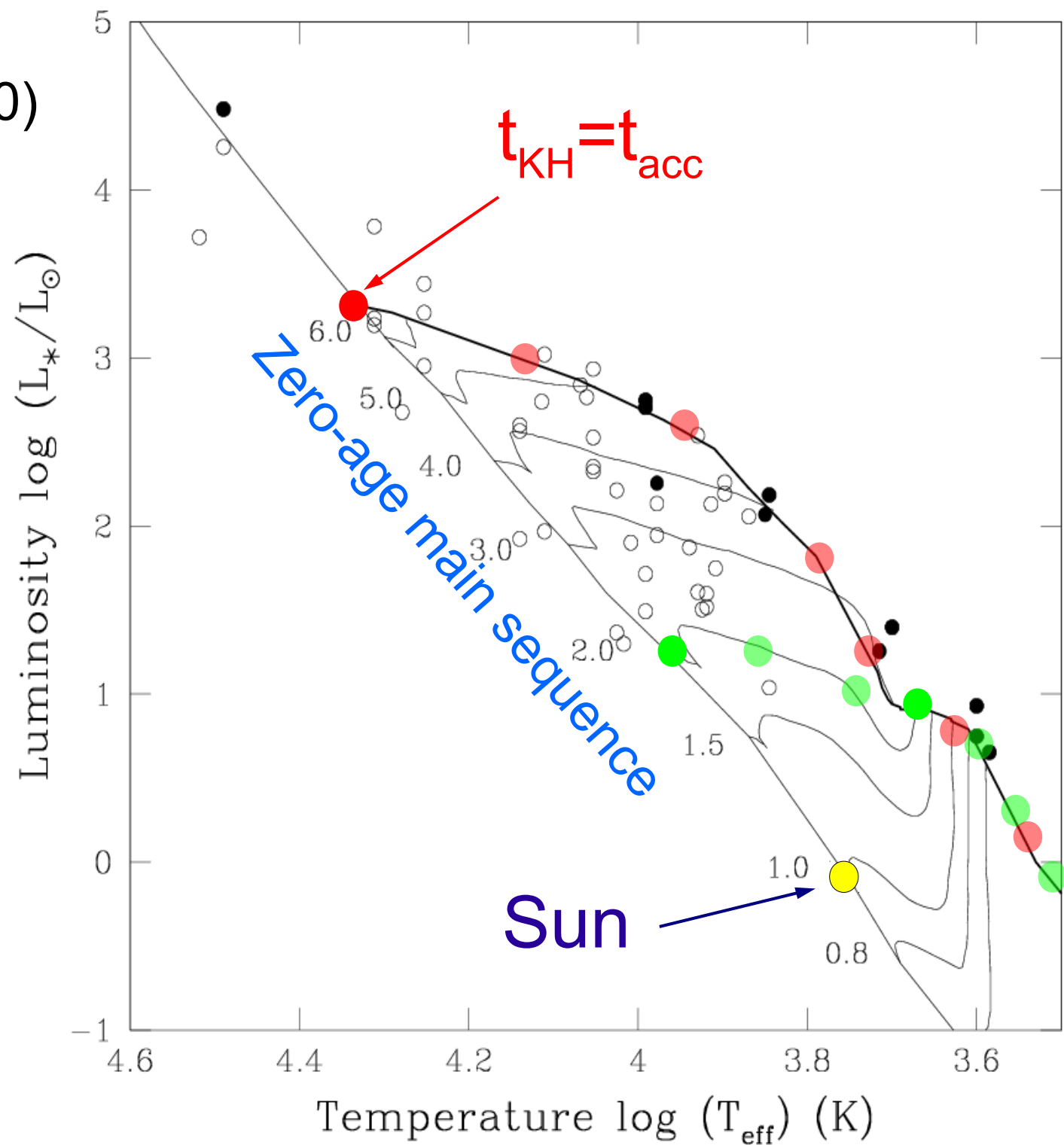
# Mass-dependence of collapse



Palla & Stahler (1990)

$$dM/dt = 10^{-5} M_{\odot}/\text{yr}$$

Massive stars  
are born on the  
Main Sequence!



# The contraction process

- The protostar becomes a pre-main-sequence star when the accreting material surrounding it is exhausted.
- The further evolution of the star, now at almost fixed mass, is driven by radiation from its surface layers.
- Quasi-static evolution of the core:

$$L = -\frac{dE_{\text{tot}}}{dt} = -\frac{d(U+W)}{dt} \text{ with } 2U+W=0 \text{ (virial) and } W = -f \frac{GM^2}{R}$$

$$L = -\frac{1}{2} \frac{dW}{dt} = -\frac{1}{2} f \frac{GM^2}{R^2} \frac{dR}{dt}$$

$f = 6/7$  for polytropic  
gas with  $\gamma=5/3$

$$L > 0 \Rightarrow \frac{dR}{dt} < 0 \quad \text{Radiative losses at the photosphere}$$

lead to gravitational contraction

$$\frac{dU}{dt} = L > 0 \quad \text{Radiative losses lead to increase of temperature!}$$

(a pre - main - sequence star is an object with negative heat capacity)

# The contraction process

Comparing timescales :

- Contraction takes place on the Kelvin - Helmholtz timescale :  $\frac{dR}{dt} \propto \frac{R}{\tau_{KH}}$  where  $\tau_{KH} \approx \frac{GM_*^2}{R_* L_*}$
- Readjustment of the hydrodynamical equilibrium through pressure waves with timescale :

$$t_s \equiv \frac{R_*}{a_s}, \text{ where } a_s = \sqrt{\frac{\gamma GM_*}{3R_*}} \text{ is the sound speed}$$

$\frac{t_s}{\tau_{KH}} \ll 1$  for pre - main - sequence stars at the birthline (and decreases as contraction proceeds)  $\Rightarrow$  the evolution is *quasi - static*

# Basic equations

Stellar structure equations in spherical symmetry:

- $dP/dr = -\rho(r) G m(r) / r^2$       Hydrostatic equilibrium
- $dm/dr = 4\pi r^2 \rho$       Mass conservation
- $P \sim \rho^\gamma$       Equation of state  
(adiabatic for convective star; ideal gas:  $\gamma=5/3$ )



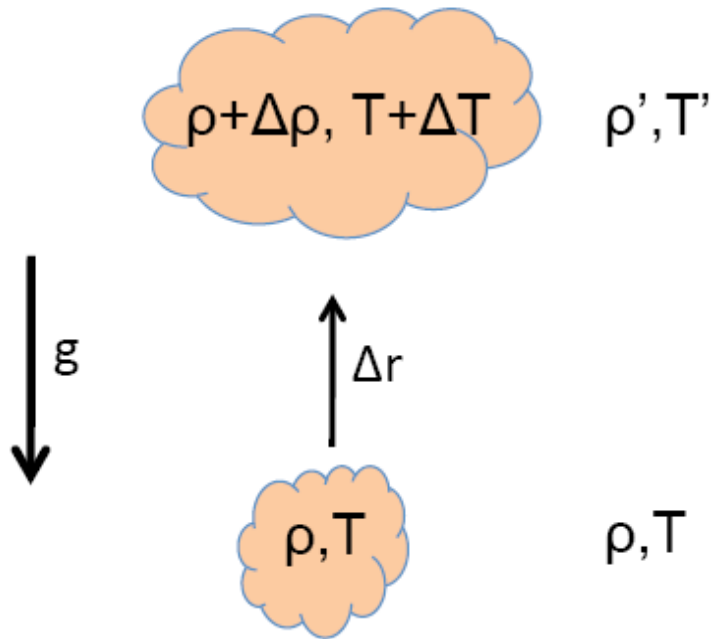
# Basic equations

Stellar structure equations in spherical symmetry:

- Energy transport:
  - ✓ if radiative:  $dT/dr|_{\text{rad}} = -3\kappa_R \rho / (64 \pi \sigma r^2 T^3) L(r)$ 
    - diffusion equation,
    - $\kappa_R$  the mean Rosseland opacity (integrated over frequency range)
  - ✓ if  $dT/dr|_{\text{rad}} > dT/dr|_{\text{adiab}}$  then
    - Creation of “hot bubbles”
    - Induction of *convection*

# Onset of convection

Principle of convection:



If moving *adiabatically* a cell of gas opposite to the gravitational acceleration results in  $\rho + \Delta\rho > \rho'$ , then the cell will fall down again.  
→ radiative stability

Radiative stability if  $\left| \frac{d\rho}{dr} \right|_{rad} < \left| \frac{d\rho}{dr} \right|_{adiab}$

or equivalently  $\left| \frac{dT}{dr} \right|_{rad} < \left| \frac{dT}{dr} \right|_{adiab}$

In the opposite case, we have convective instability: the heat is transported by movement of material instead than by matter.

# Convection

- Turn-over happens extremely fast:  $< 1a$ 
  - Energy transport is done through *convection*
  - Creates relatively uniform temperature
  - Stable configuration with  $T_{\text{eff}} \sim 3500\text{-}4000\text{K}$
- → Continuation of isothermal collapse  
(that lead to the formation of the 2<sup>nd</sup> hydrostatic core)

# Initial conditions

- Size of 2<sup>nd</sup> hydrostatic core:
  - Determined by end of 2<sup>nd</sup> collapse
  - Determined by energy consumed by dissociation and ionization

$$E_{int} = \frac{M_{\star}}{m_H} \left[ X_H \left( \frac{E_{diss}(H_2)}{2} + E_{ion}(H) \right) + X_{He} \frac{E_{ion}(He)}{4} \right]$$

- $X_H=0.7$ ,  $X_{He}=0.28$
- $E_{ion}(H)=13.6\text{eV}$ ,  $E_{ion}(He)=78.98\text{eV}$ ,  $E_{diss}(H_2)=4.48\text{eV}$

$$E_{int} = 3.17 \times 10^{39} J \frac{M}{M_{\odot}}$$

# Initial conditions

- Size of 2<sup>nd</sup> hydrostatic core:
  - Determined by energy consumed by dissociation and ionization

$$E_{int} = \frac{1}{2} W_{\text{collapse}} = \frac{GM^2}{2R_{2.\text{core}}} - \frac{GM^2}{2R_{1.\text{core}}} \approx \frac{GM^2}{2R_{2.\text{core}}}$$

- Resolve for  $R_{2.\text{Core}}$ :  $R \approx 60 \frac{M}{M_{\odot}} R_{\odot}$
- **Problem:**
  - Cores should be resolvable – not seen so far  
→ R must be smaller by factor >5
  - Explanations:
    - Too deeply embedded (?)
    - Quick continued collapse → energy problem

# Temperature

- Temperature:

- Assume virial equilibrium

Internal energy  $U = \frac{3}{2} k T \frac{M}{\mu}$

takes half of gravitational energy  $W = -\frac{GM}{R}$

$$T = \frac{\mu}{3k} \frac{GM}{R} = 850 [\text{K}] \left( \frac{M}{0.05 M_{\odot}} \right) \left( \frac{R}{5 \text{ AU}} \right)^{-1}$$

- $T_{\text{eff}} = 5000\text{-}10000\text{K}$

- In agreement with accretion temperature

- Observed: 3500-4000K

- Explains only small fraction of radius discrepancy

# Luminosity

- How does the collapse energy reach the surface?
- Radiative transfer:
  - Opacity of ionized medium:  $\kappa_R \propto \rho^n T^{-s}$ 
    - Free-free transitions  $H^+-e^-$ :  $n=1, s=3.5$   
Kramer's opacity – relevant in most of the core
    - $H^-$  ions (electrons from metals):  $n=1/2, s=-9$   
relevant in cool outer layers
- Radiative transport:  
$$L(r) = (64 \pi \sigma r^2 T^3 / 3 \kappa_R \rho) (-dT/dr)$$
- Maximum luminosity for radiative transport

# Luminosity

- Maximum luminosity for radiative transport
- Constrained by stability against convection:

$$|dT/dr|_{\text{rad}} < |dT/dr|_{\text{adiab}}$$

- Max radiative luminosity:

$$L_{\text{rad,max}} = \alpha \mu M(r) T^3 / (\kappa_R \rho)$$

$$L_{\text{rad}} \approx (M/M_{\odot})^{3+s-n} (R/R_{\odot})^{s-3n}$$

- Energy that can be radiatively transferred is in the order of  $1L_{\odot}$
- Actual luminosity:  $> 10^2 L_{\odot}$

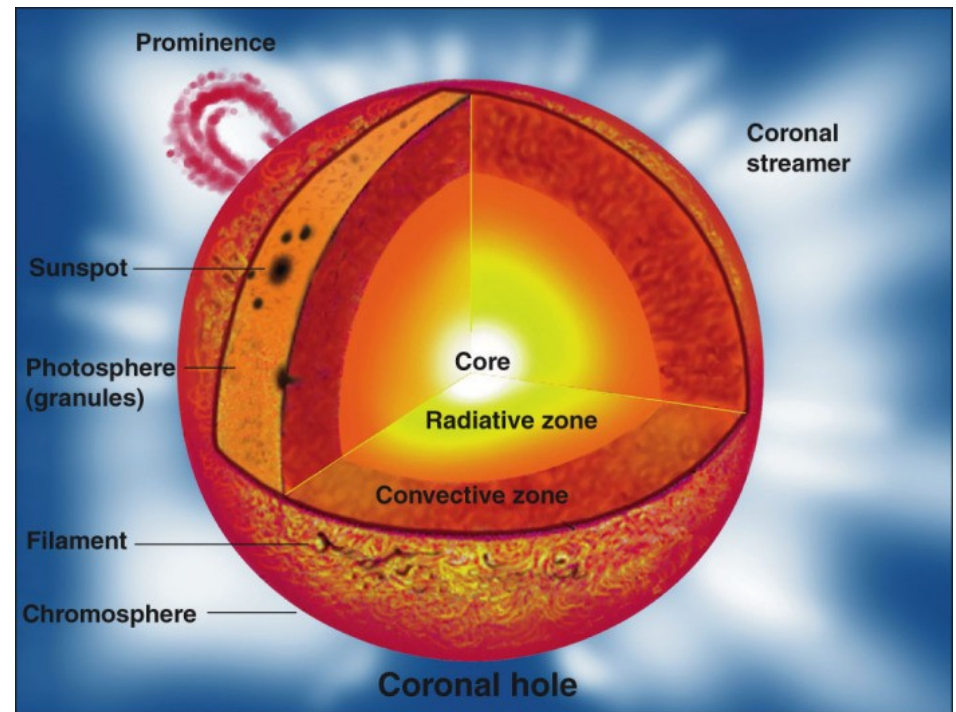


# Luminosity

- Only small fraction of collapse energy can be transferred radiatively
- Max radiative luminosity:

$$L_{\text{rad,max}} = \alpha \mu M(r) T^3 / (\kappa_R \rho)$$

- Convection is favored at low masses, low  $T$  and/or high opacities
- Radiative zone only in the centre of massive PMS's



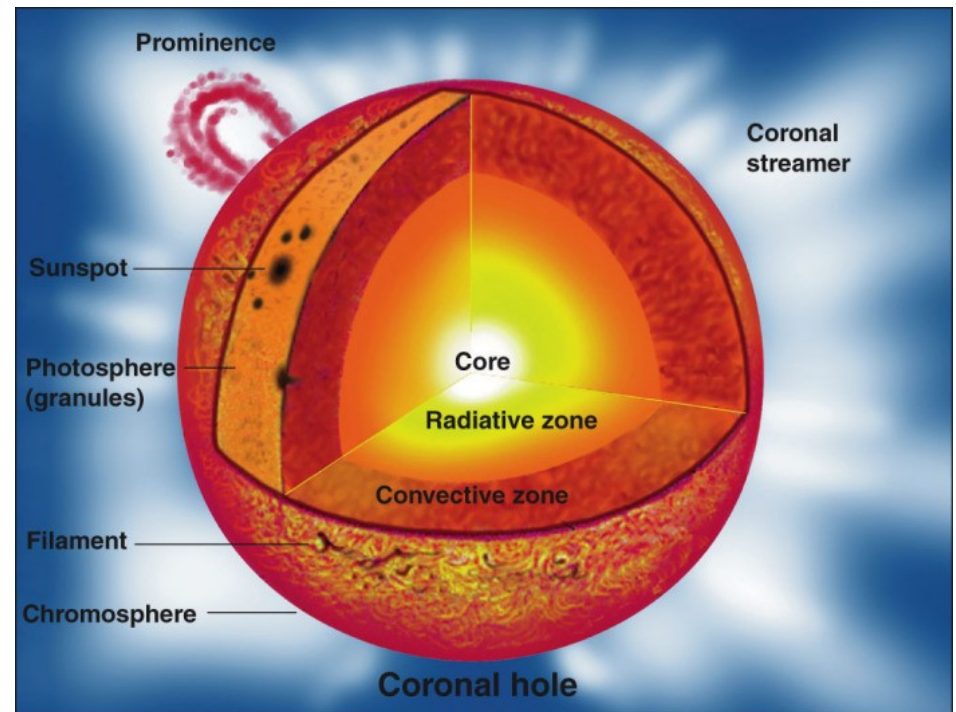
# Temperature

- End of radiative zone defines temperature of convective zone

$$T_{\text{eff}} \sim M^{4/5} L^{1/5} \quad \text{for Kramer opacity}$$

$$T_{\text{eff}} \sim M^{7/31} L^{1/102} \quad \text{for H}^- \text{ opacity}$$

- At the lower edge of the convective zone, determined by H<sup>-</sup> opacity, the temperature is very constant, almost independent of luminosity



Courtesy of Encyclopaedia Britannica, Inc.; illustration by Anne Hoyer Becker, from "A New Understanding of Our Sun," by Jay M. Pasachoff, 1989 Britannica Yearbook of Science and the Future

# Convective contraction: Hayashi tracks

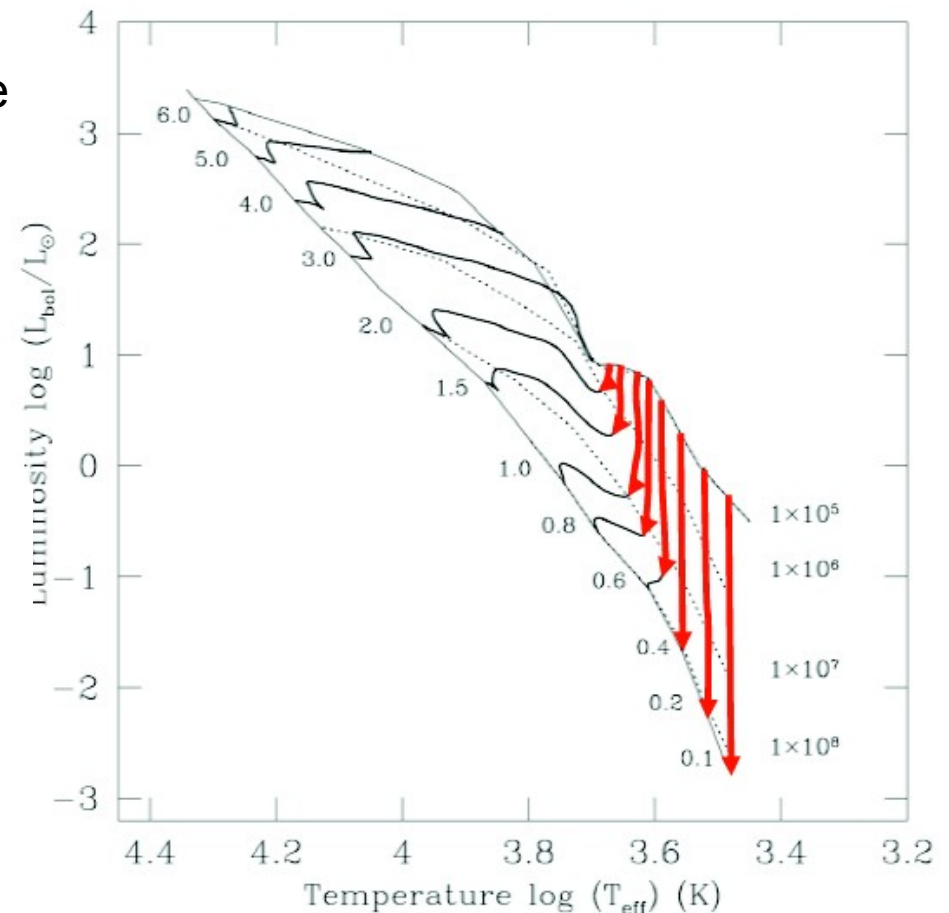
Contraction at almost constant  $T_{\text{eff}}$

- At  $T < 3500\text{K}$ , the opacity in the photosphere (dominated by  $\text{H}^-$ ) drops very quickly with decreasing temperature.
- $F_{\text{photosphere}} = F_{\text{conv}} \rightarrow$  opacity should be high enough
- $\rightarrow T$  cannot be lower than the so-called *Hayashi temperature*

$$L_* = -\frac{dE_{\text{tot}}}{dt} = -\frac{3}{7} \frac{GM_*^2}{R_*^2} \frac{dR_*}{dt}$$

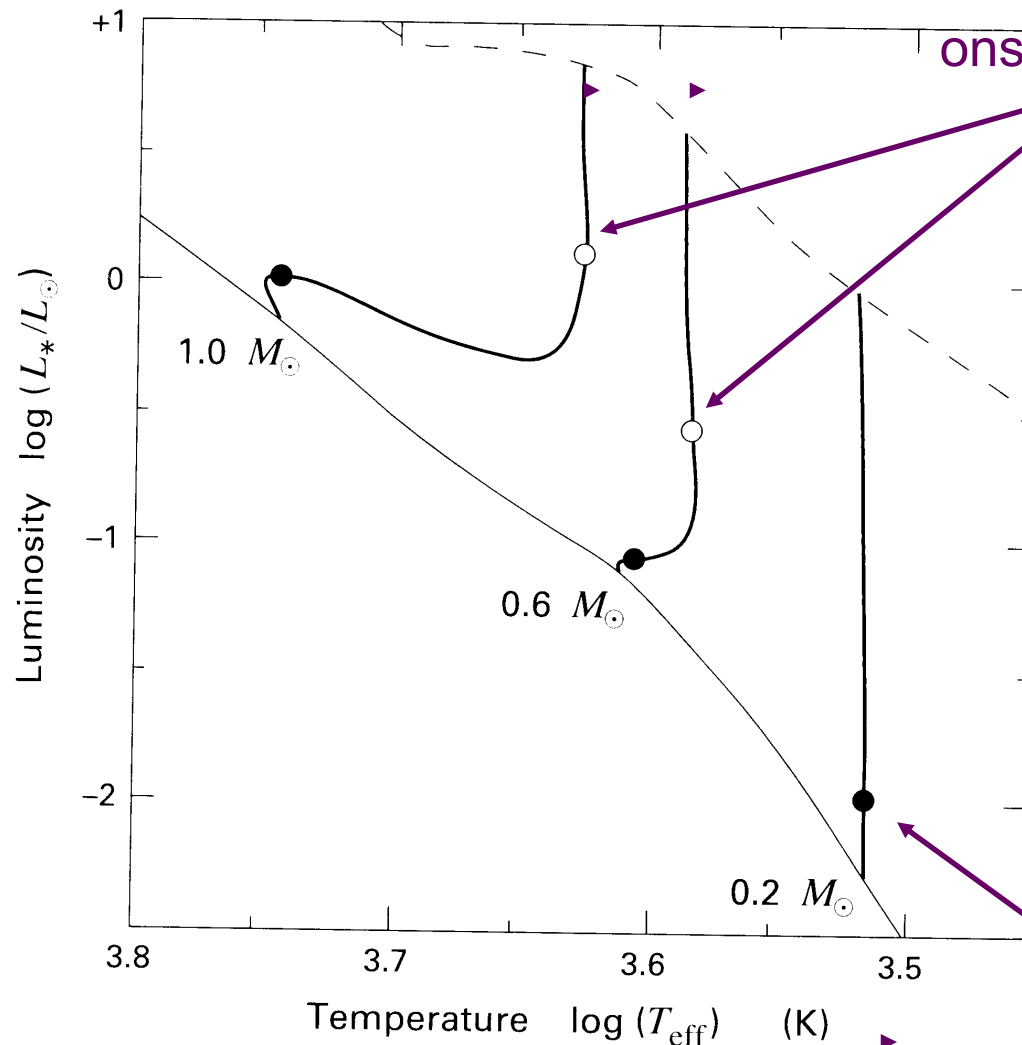
$$T_{\text{eff}} = \left( \frac{L}{4\pi R_*^2 \sigma} \right)^{1/4} \approx \text{constant}$$

$$\Rightarrow L_* = L_0 \left( \frac{3t}{\tau_{\text{KH}}} \right)^{-2/3}, \text{ where } \tau_{\text{KH}} = \frac{3}{7} \frac{GM_*^2}{R_0 L_0}$$



# Formation of a radiative core

relevant for upper low-mass PMS stars ( $0.6M_{\odot} \leq M_{*} \leq 2M_{\odot}$ )



onset of radiative stability

- ▶ When  $T$  increases ( $T_c \sim M/R$ ), opacity decreases (dominated by free-free for higher temperature range)

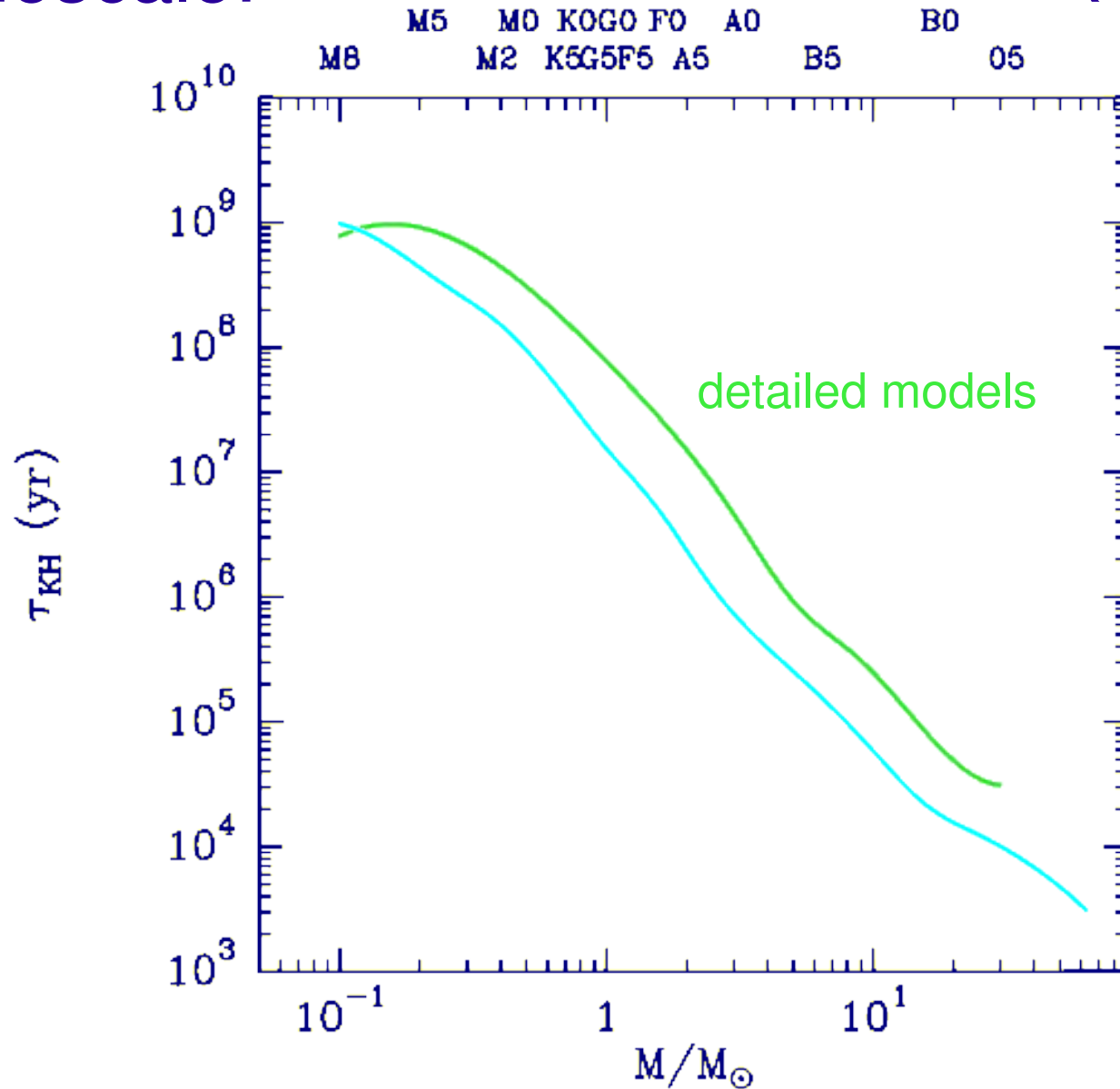
$L_{\text{rad,max}} \sim T^3/k\rho$   
→  $L_{\text{rad,max}}$  increases  
→ becomes radiative

start of hydrogen burning

# Radiative energy transfer

K-H Timescale:

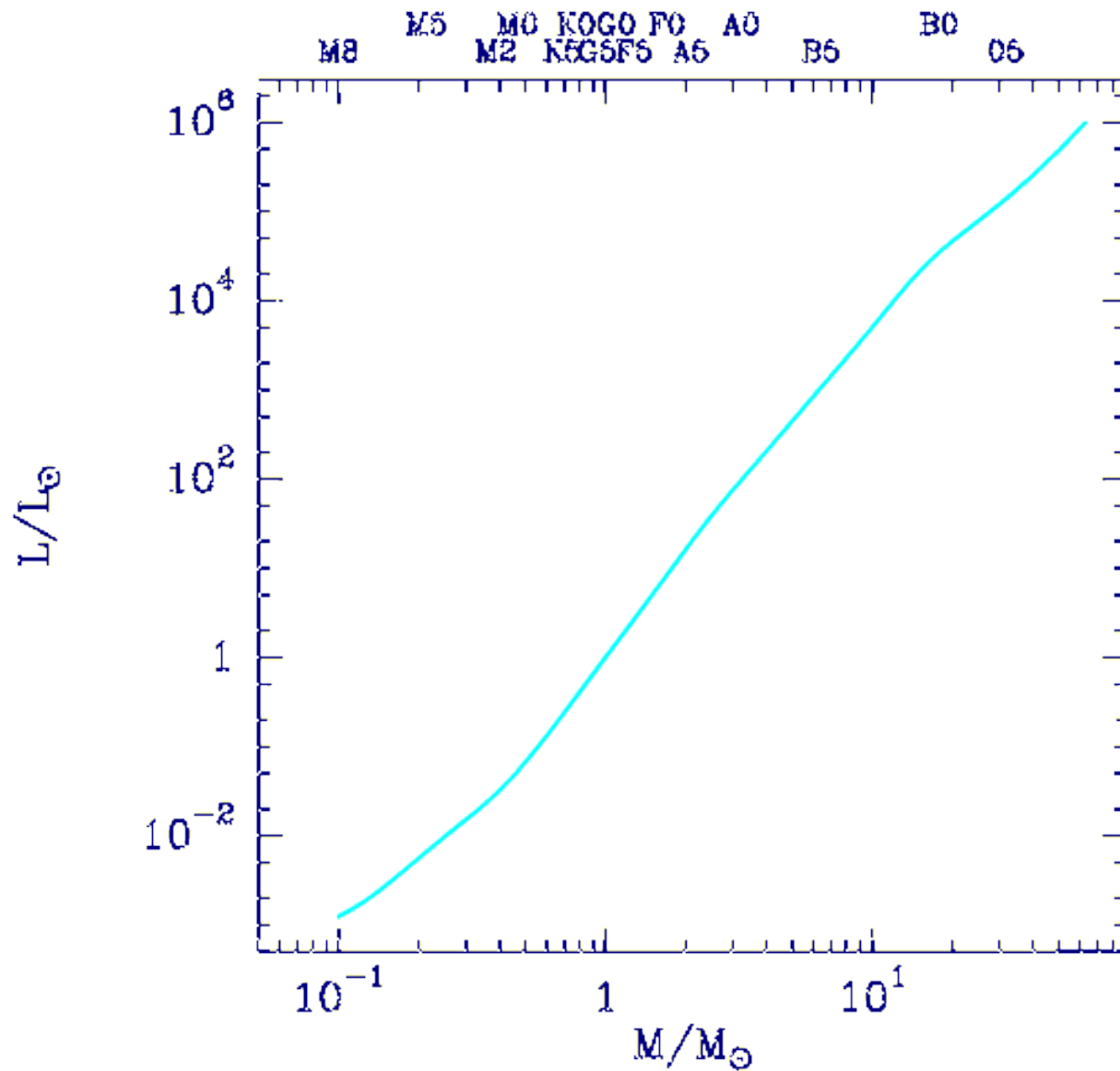
$$\tau_{KH} \propto M^{-9/5}$$



# Luminosity

- Feed by collapse  $L = \frac{1}{2} \frac{dW}{dt} = -\frac{GM^2}{2R^2} \frac{dR}{dt}$
- Contraction time determined by Helmholtz-Kelvin timescale
$$\tau_{HK} = \frac{1}{dR/dt}$$
- Resolve for L:  $L \propto R^{-5/2}$

# Mass-Luminosity Relation: $L \propto M^{3.2}$



Mass-Radius relation:  $R \propto M^{0.6}$

# Luminosity

- Luminosity-size relation:  $L \sim R^{-5/2}$
- Use blackbody radiator:  $L = 4\pi R^2 \sigma T_{eff}^4$

$$\rightarrow T_{eff} \sim R^{-9/8}$$

$$\rightarrow L \sim T_{eff}^{20/9}$$

- = Henyey-track



# HR diagram

Transition from  
isothermal  
collapse to  
radiative core:

→ Henyey tracks

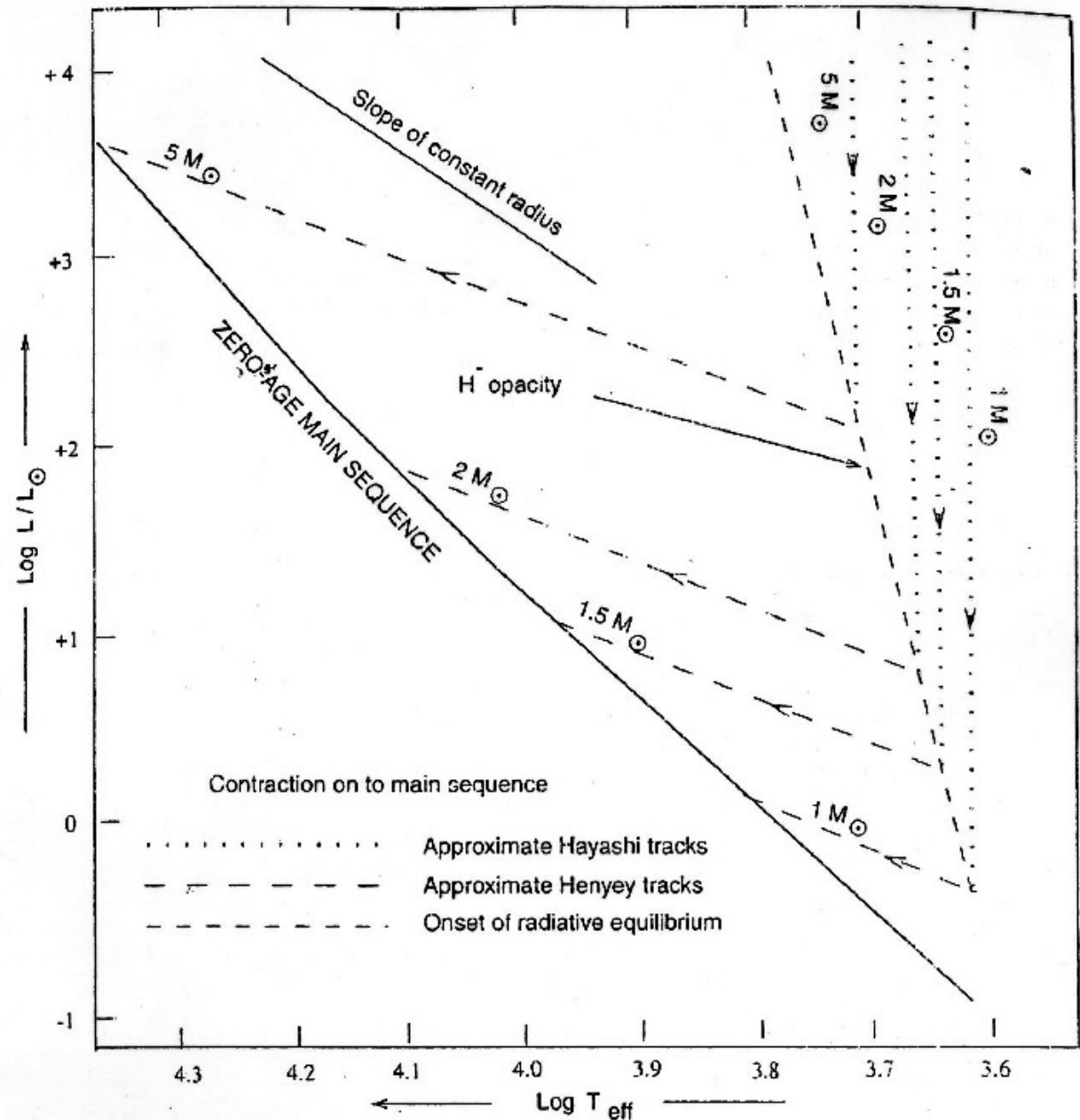


Fig. 3.3. The late stages in the collapse of a protostellar cloud towards the main sequence corresponding to the path EFG of Fig. 3.2. The nearly vertical dotted lines are the Hayashi tracks for different masses, and the sloping dashed lines are the Henyey tracks for the corresponding masses. The transition from the Hayashi to the Henyey track occurs along a line that is determined by the nature of the opacity. The line marked  $H^{-}$  opacity illustrates this transition.

# Radiative contraction: Heney tracks

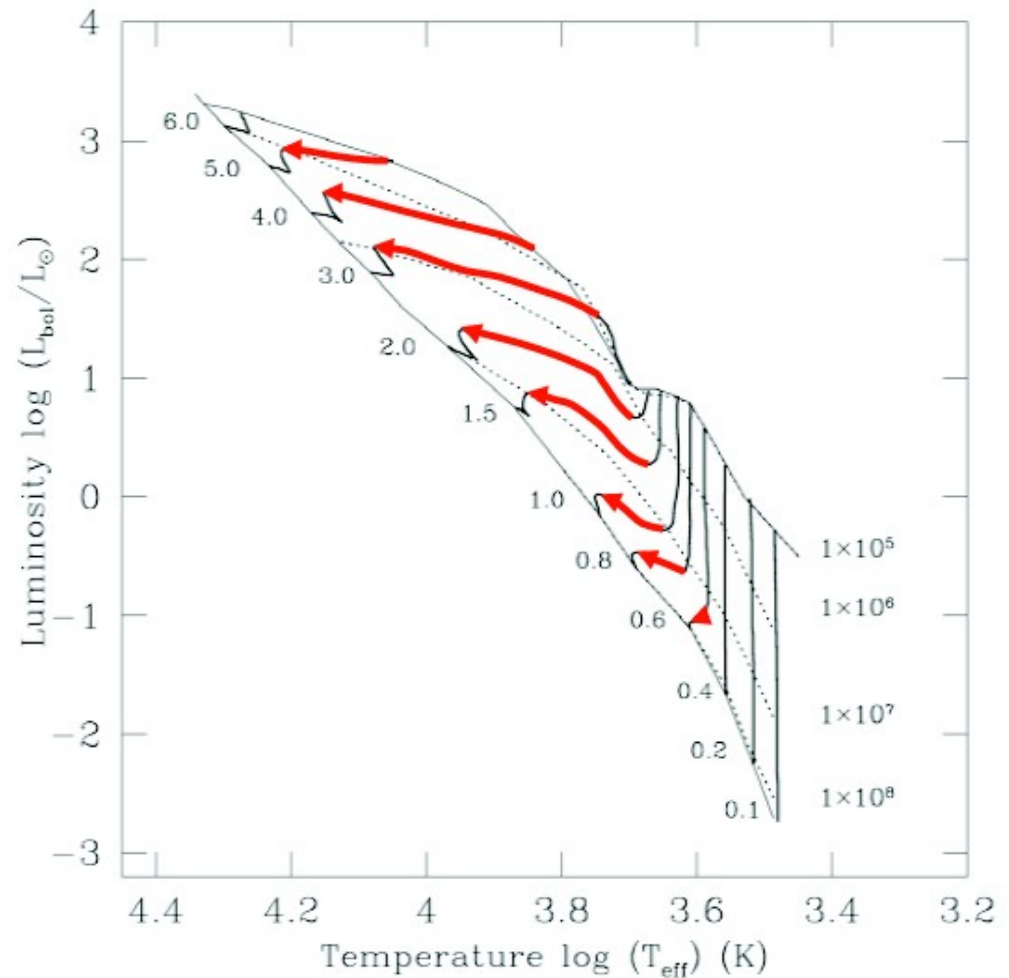
- for low- to intermediate- mass PMS stars ( $0.6M_{\odot} \leq M_{*} \leq 8M_{\odot}$ )
- Radiative stars have a well-defined mass-luminosity relationship:

$$L(r) = \frac{16\pi\sigma R^2}{3\kappa_R\rho} \left( -\frac{dT^4}{dR} \right)$$

$$\Rightarrow L \propto \langle \kappa_R \rho \rangle^{-1} R T^4$$

$$\text{with } T \propto M/R \text{ and } \langle \rho \rangle \propto M/R^3$$

$$\Rightarrow M^3 \langle \kappa_R \rangle^{-1} \propto L$$

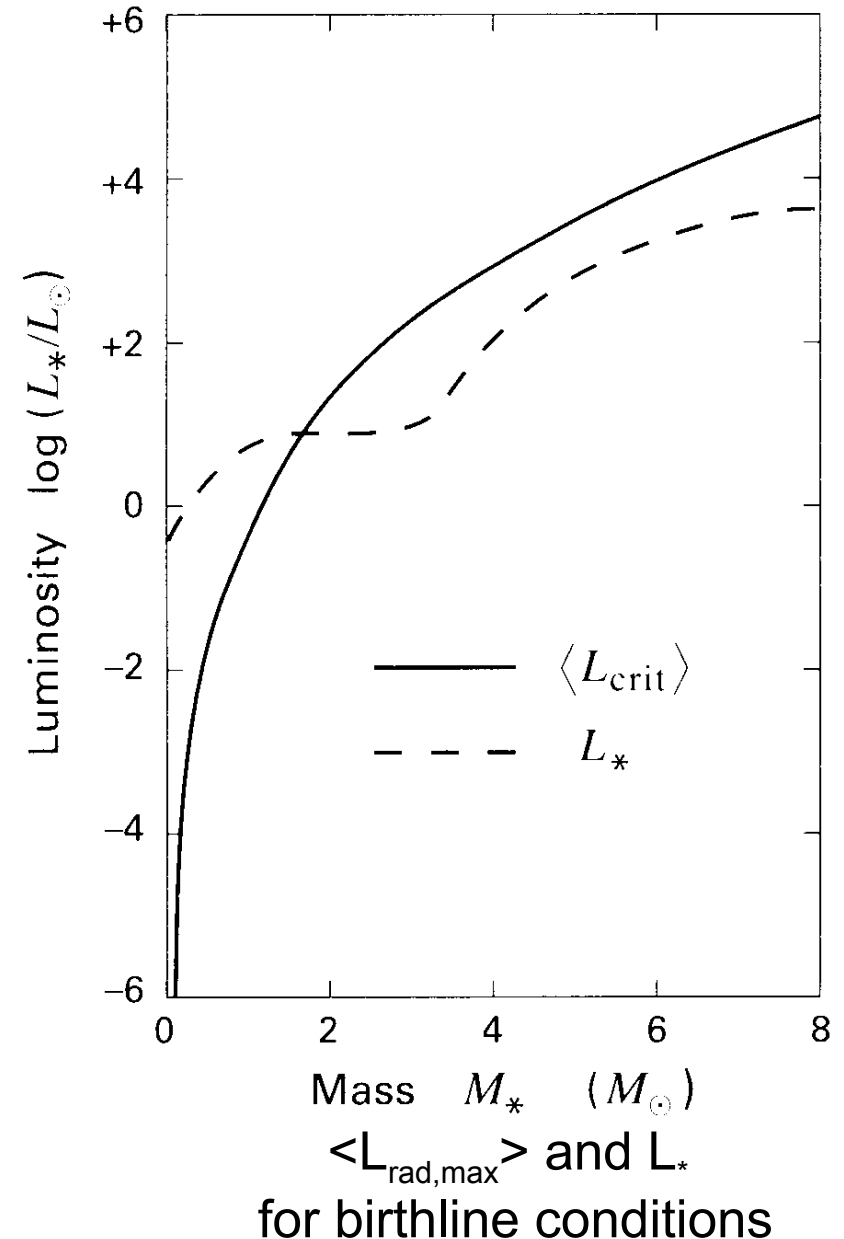


# Global picture (for low-mass PMS)

- Start with isothermal collapse → Hayashi track
  - Luminosity dominated by accretion
- End of main accretion phase
  - Luminosity dominated by adiabatic contraction
- Fully convective core
  - continuation of Hayashi track
  - Temperature limited by Hayashi temperature ( $H^-$  opacity temperature)
- Increase of temperature to allow  $L_{\text{rad,max}} > L$ 
  - Radiative transfer of luminosity
  - Reduced stellar contraction
  - Henyey track up to ignition

# Mass-dependence of evolutionary tracks

- Very low-mass PMS stars ( $M_* \leq 0.6M_\odot$ ):
  - ✓ The star is fully convective throughout the contraction process
- Low-mass PMS stars ( $0.6M_\odot \leq M_* \leq 2M_\odot$ ):
  - ✓ Star fully convective at the beginning of contraction
  - ✓ Appearance of a radiative core
  - ✓ Radiative contraction at the end
- Intermediate-mass PMS stars ( $2M_\odot \leq M_* \leq 8M_\odot$ ):
  - ✓ Radiative contraction
- High-mass PMS stars ( $8M_\odot \leq M_*$ ):
  - ✓ Do not exist!



# Mass-dependence of evolutionary tracks

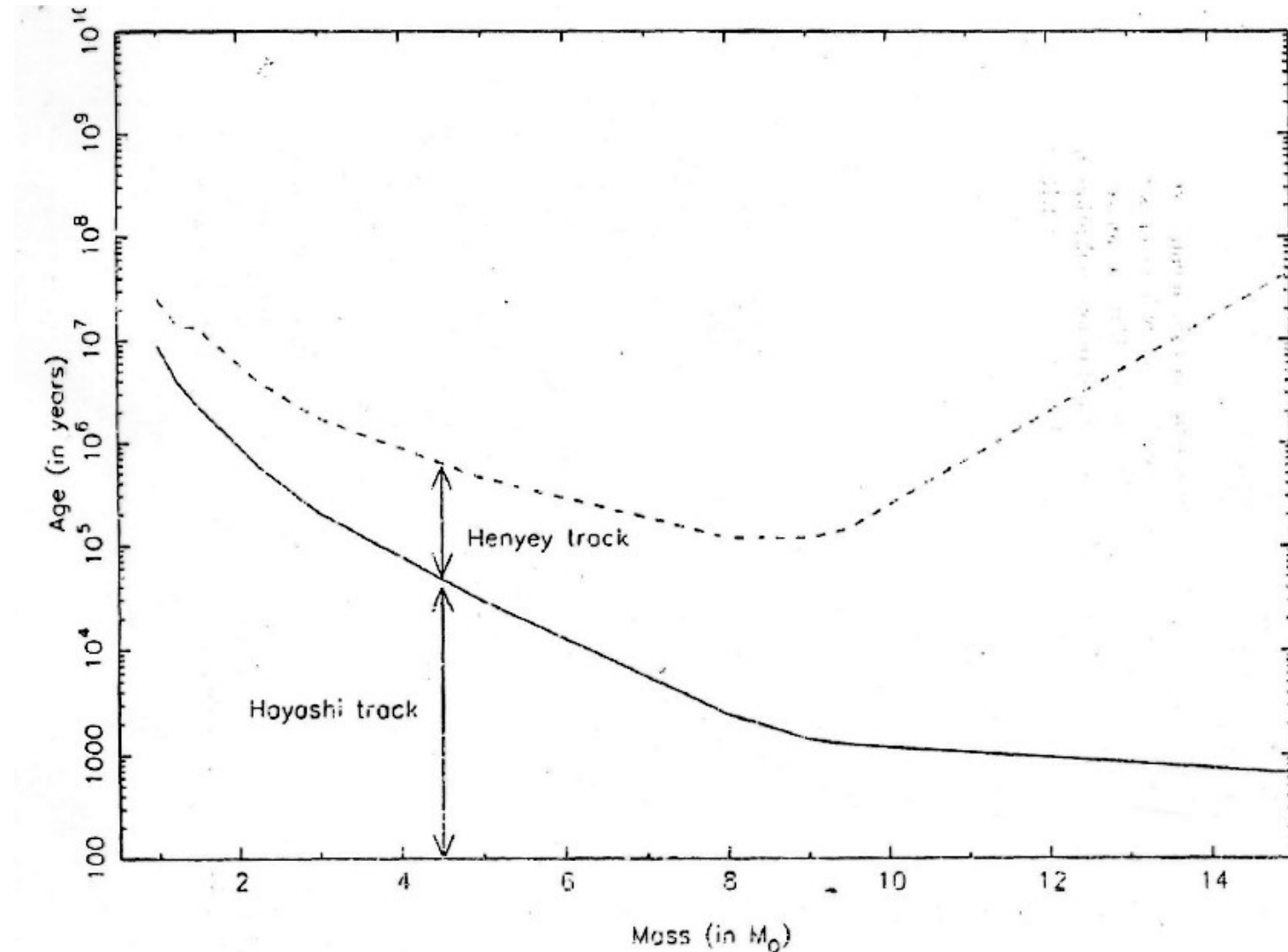


Fig. 3.4. Time spent by stars of different masses in the Hayashi and the Henyey tracks. High-mass stars spend less time on the Hayashi track, and more on the Henyey track, as is clear from Fig. 3.3 as well.

# Observational use of the HR diagrams

Derive the age and mass of the PMS stars from their position on the HR diagrams. Especially powerful for star-forming clusters, for which relative distance uncertainties are lower.

Goals and (still) open questions:

- look into evolution of disks, in the planet formation era  
(later T Tauri phase).

Time decay of disk accretion?

- derive history of star formation

# Example of Taurus-Auriga

Taurus-Auriga is a low-extinction star-forming region.

How to determine  $L$  and  $T_{\text{eff}}$  from observations?

- $T_{\text{eff}}$ : spectral type can be determined by ratio of strength of photospheric absorption lines

- $L$ : observed fluxes have to be corrected for interstellar extinction, and converted into absolute fluxes after the distance has been determined

Medium age  $\sim 10^6$  yrs

Some WTTS closer to the main sequence (=older).

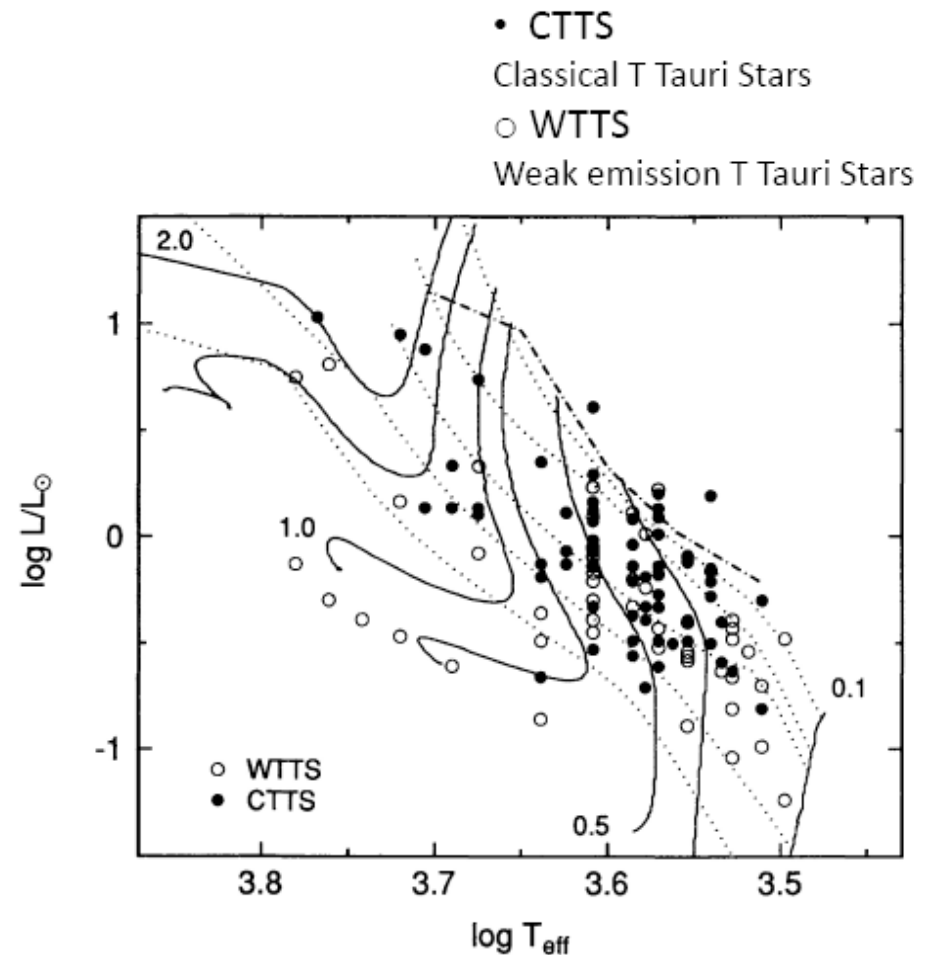


FIG. 15.—H-R diagram for Taurus-Auriga TTSs. Solid lines indicate CMA model tracks for  $M_{\star} = 0.1, 0.3, 0.5, 0.8, 1.0, 1.5, \text{ and } 2.0 M_{\odot}$  (D'Antona & Mazzitelli 1994). Several tracks are labeled with their mass. Dotted lines denote isochrones for  $10^5, 3 \times 10^5, 10^6, 3 \times 10^6, \text{ and } 10^7$  yr. The heavy dot-dashed line indicates the stellar birth line (Fletcher & Stahler 1994a, Table 1).

Kenyon et al. 1995

# Uncertainties

- In the models:
  - ✓ energy transport at the frontier between radiative and convective zones (treatment of convection in the radiation dominated zones by the “mixing-length” parametric method)
  - ✓ opacities: difficult to compute from thousands of spectral lines
- On the observational side:
  - ✓ Correction for interstellar and circumstellar absorption
  - ✓ Distance determination
  - ✓ Contribution of accretion luminosity
  - ✓ Factors of 2 to 3 on ages and masses...



# Conclusions

- PMS evolution depends on the mass:
  - ✓ very low mass stars remain convective during the whole evolution
  - ✓ low-mass stars start convective and then develop a radiative core
  - ✓ intermediate-mass stars are radiative
  - ✓ high-mass stars don't have a PMS evolution (they are born adults!)
- HR diagram useful to study stars and PMS
  - ✓ convective contraction as vertical tracks: Hayashi tracks
  - ✓ radiative contraction as horizontal tracks: Henyey tracks
  - ✓ observationally positioning PMS stars in the HR diagram allow to determine age and mass (using the modelled tracks)... but with uncertainties of a factor of a few.